Nuclear Engineering and Design 266 (2014) 70–77

Contents lists available at ScienceDirect

Nuclear Engineering and Design

journal homepage: www.elsevier.com/locate/nucengdes

Coupling between mechanical and transfer properties and expansion due to DEF in a concrete of a nuclear power plant

Mohamad Al Shamaa[a,b], Stéphane Lavaud[a], Loic Divet[a], Georges Nahas[b], Jean Michel Torrenti[a,*]

[a] Université Paris-Est, IFSTTAR, France
[b] Institut de Radioprotection et de Sûretée Nucléaire (IRSN), 31 avenue de la Division Leclerc, 92260 Fontenay-aux-Roses, France

HIGHLIGHTS

- We model the thermal behavior of a nuclear vessel during its construction.
- We follow the expansion of concrete samples that have followed a representative thermal history.
- We examine the evolution of expansion and of the microstructure and mechanical properties of theses samples.
- The permeability of these samples is strongly affected by expansion.

ARTICLE INFO

Article history:
Received 27 April 2013
Received in revised form 7 October 2013
Accepted 14 October 2013

ABSTRACT

This paper focuses on studying the consequences of expansion due to delayed ettringite formation (DEF) on transfer and mechanical properties of concrete in the case of nuclear structures. It concerns a concrete representative of a containment vessel of a nuclear power plant where temperature variations at early age are very large. An experimental heat treatment, representative of the temperature history in the raft foundation of the containment vessel was reproduced after a modeling of its temperature rise. After this treatment, concrete exhibits swelling due to the development of DEF. The gas permeability is increased significantly after swelling, and the safety requirements expected by these structures are thus affected.

1. Introduction

Delayed ettringite formation in concrete structures is a pathology that can develop when special conditions on the composition of concrete, the thermal conditions at early age and environmental conditions are met. This phenomenon develops in concrete where temperature at early age is large, and it is mainly found in structures that are in contact with a moist environment for several years (Divet, 2001). It can affect two types of concrete: concrete heat-treated and concrete cast in place in massive parts. In the case of massive pieces, some cases of DEF were detected (Divet, 1998, 2001; Barbarulo, 2002; Baghdadi, 2008). Indeed, the temperature rise in a concrete member depends on the exothermicity of the concrete but also on its geometry, the initial temperature of the material and the heat loss. When the concrete elements are not voluminous, the heat losses to the outside are important, and the temperature in the core of the concrete part remains close to that in the exterior. On the other hand, in the case of a massive part, the heat generated by cement hydration is higher than heat losses. The temperature in the core of the piece of concrete can reach values larger than 65 °C. In general, a minimum temperature of about 65–70 °C is necessary for appearance of DEF (Heinz and Ludwig, 1987; Lawrence, 1995, 1999; Odler and Chen, 1995; Kelham, 1996; Shayan and Ivanusec, 1996; Scrivener et al., 1999; Zhang et al., 2002; Petrov and Tagnit-Hamou, 2004; Barbarulo et al., 2005; Brunetaud, 2005; Tosun, 2006; Hanehara et al., 2008a, 2008b). But this temperature is highly dependent on the duration of its application. The development of DEF is manifested by swelling and cracking of the concrete.

In the nuclear field, the evaluation of pathologies in concrete of nuclear structures represents an essential issue for the nuclear safety, especially in containment vessels which are very massive concrete structures and which represent the third and final safety barrier of the reactor. Indeed, some pathologies, such as DEF, could damage the concrete of these structures, and thus the security requirements expected could be under threat, especially those responsible of the mechanical behavior (strength, stability of structural elements) and the tightness. Compliance with these requirements is assessed against criteria defined according

* Corresponding author. Tel.: +33 1 81 66 84 40; fax: +33 1 81 66 89 90.
E-mail addresses: jean-michel.torrenti@ifsttar.fr, jean-michel.torrenti@ponts.org (J.M. Torrenti).

0029-5493/$ – see front matter © 2013 Elsevier B.V. All rights reserved.
http://dx.doi.org/10.1016/j.nucengdes.2013.10.014

to different operating situations established by the safety analysis. Confidence in the value of these criteria assumes control of their evolutions over time. It should also be noted that reinforced and prestressed concrete nuclear structures, such as containment vessels, are among the elements which can not be replaceable. Therefore, they must be in an acceptable service state until the end of exploitation.

In France, 24 reactors are provided with vessels called double wall. They consist of a prestressed concrete wall and a reinforced concrete wall separated by a space. There is no metallic liner in these containments. So concrete is the material that must ensure airtightness. And the consequences of swelling due to DEF on the permeability of concrete and on the airtightness of the containment still remain unknown.

Thus it appears necessary for nuclear structures to ascertain whether there is any likelihood of long-term development of DEF, and to study if its consequences on the permeability of the concrete can affect severely the durability of the containment. Therefore, in this paper, the evolution of temperature fields at early age in the raft foundation of a containment vessel is modeled. Then, an experimental program is applied in order to assess the risk of developing a DEF. In addition, the effects of DEF on mechanical and transfer properties of the concrete are measured and analyzed.

2. Thermal simulation

These simulations have been performed to predict temperature fields created during the first hours after the casting of the concrete during the construction of the raft. The finite element model used is that developed by (Benboudjema and Torrenti, 2008).

2.1. Chemo-thermal model

The evolution of the temperature of the concrete is obtained by solving the energy balance equation that includes the release of heat due to the hydration reaction:

$$C\dot{T} = \nabla(k\nabla T) + L\dot{\xi} \quad (1)$$

in which ξ is the rate of degree of hydration, T is the temperature [K], k is the thermal conductivity [W m^{-1} K^{-1}], L is the latent heat of hydration [J m^{-3}] and C is the volumetric heat capacity [J m^{-3} K^{-1}] which could be considered constant (Waller, 2000).

Then, we use an Arrhenius type law in a notation proposed by Ulm and Coussy (1998), to take into account a thermo-activated process due to the hydration of cement paste:

$$\frac{d\xi}{dt} = \tilde{A}(\xi)\exp\left(\frac{-E_a}{RT}\right) \quad (2)$$

in which E_a is the activation energy [J mol^{-1}], R is the constant of perfect gas 83,145 J K^{-1} mol^{-1} and C is the normalized affinity given by:

$$\tilde{A}(\xi) = a + b\xi + c\xi^2 + d\xi^3 + e\xi^4 + f\xi^5 + g\xi^6 \quad (3)$$

in which a, b, c, d, e, f and g are parameters identified from a quasi-adiabatic test on a concrete mixture whose formulation is the same of that used in nuclear structures (Briffaut et al., 2011).

The boundary conditions are assumed to be of convective type. The heat flow φ is written as follows:

$$\varphi = h(T_s - T_{ext})n \quad (4)$$

in which h is the coefficient of exchange by convection [W m^{-2} K^{-1}], T_s is the temperature on the surface [K], T_{ext} is the ambient temperature [K] and n is the normal unit vector to the surface (oriented toward the exterior).

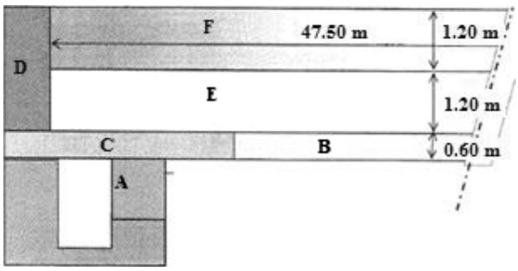

Fig. 1. Vertical section of the raft.

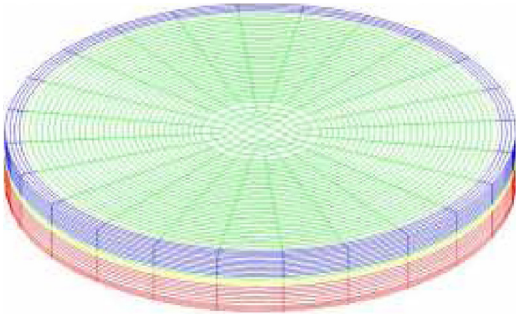

Fig. 2. Mesh of the raft foundation with different blocks of concreting.

2.2. Simulated evolutions of temperature in the raft

The raft foundation supports the containment and internal structures. It consists of a 3 m thick reinforced concrete (the subface −6.00 m) and 60 cm of concrete charging. The raft has a gallery on its periphery for anchoring the vertical tendons. It is a gallery of prestressing detached from the raft with inner dimensions of 2.20 m × 2.60 m, the level of the underside is −9.10 m. This gallery does not communicate with the space between walls, but is accessible through the manhole opening to the outside of the reactor building.

To estimate the heating cycle that existed within the raft foundation, we modeled the temperatures attained in the concretes during the construction of the massive members. The finite elements calculations were solved and constructed using the finite elements code *Cast3m* developed by the French Atomic Energy Commission (CEA) (Cast3m, 2009). Casting was done in six blocks A, B, C, D, E, and F (Fig. 1). A 3D modeling is realized (Fig. 2). The input parameters of this simulation are presented in Table 1. The calculations take into account a realistic phasing of the casting: each block of concrete is divided into layers, so that each layer is cast in a period of 1 h. The speed of the casting is 100 m^3/h. The outside temperature is taken

Table 1
Parameter values used in simulations.

Parameter	Value
$\rho_{concrete}$	2423 kg/m^3
C	2400 kJ/(°C m^3)
K	2.8 W m^{-1} K^{-1}
E_a	45,729.75 J mol^{-1}
R	8.3145 J K^{-1} mol^{-1}
h	12.5 W m^{-2} K^{-1}
L	117,840 kJ m^3
a	64.417
b	18,042
c	−94,620
d	215,819
e	−280,339
f	208,172
g	−67,901

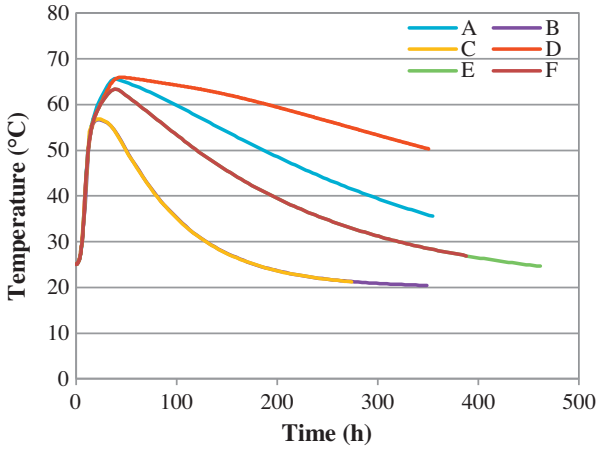

Fig. 3. Maximum simulated evolutions of temperature of concrete in all blocks of the raft.

equal to 20 °C and the initial temperature of concrete to 25 °C. Based on these data, the maximum evolutions of the temperature of the concrete in all the blocks are shown in Fig. 3. The results show that some blocks undergo significant heating, especially the blocks A, D, E and F where the maximum temperature exceeds 60 °C. The critical evolution is at a point situated in the core of the block D. At this point, the concrete reaches a temperature equal to 66 °C after 45 h of hydration and remained at temperatures of above 60 °C for about six days. The speed of the cooling phase appears to be low. On the other hand, the heat developed in the blocks B and C is quickly released to the outside and does not cause significant elevations in temperature (due to the small thickness of these blocks).

3. Experiments

3.1. Materials and procedures

Table 2 summarizes the mix design of the concrete used in the construction of the raft foundation. Concrete is made with calcareous aggregates (in order to avoid the risk of alkali-aggregate reaction) and Portland cement CEM II/A-LL 42.5 R, which can be susceptible to an expansive behavior due to DEF. The chemical and mineralogical compositions of the cement are given in Tables 3 and 4. Concrete specimens were prepared according to the standards NF P 18-400 and NF P 18-422. Samples were cast in cylindrical molds whose dimensions are 11 cm (diameter) and 22 cm (height). After casting, a part of concrete specimens was cured according to heat treatments derived from the numerical thermal cycle followed by concrete in the block D. The maximum temperature in this cycle reaches a value of 66 °C. It was decided to increase this one in order to reach 70 °C to expose concrete to a more severe condition by taking into account the variability of the properties of the material. Indeed, Torrenti and Buffo-Lacarrière (2010) have studied the influence of some parameters on the variability of the temperature field generated by the hydration of cement in a structure of concrete at early age, especially on the maximum

Table 2
Concrete mix design.

Material	kg/m³
CEM II/A-LL 42.5 R cement	350
Calcareous sand 0/5 mm	772
Calcareous aggregate 5/12.5 mm	316
Calcareous aggregate 12.5/20 mm	784
Water	201
Plasticizer	1.225

Table 3
Chemical analyses of cement CEM II/A-LL 42.5 R.

CEM II/A-LL 42.5	Wt.%
SiO_2	19.37
Al_2O_3	4.58
Fe_2O_3	3.06
TiO_2	0.28
MnO	0.07
CaO	63.66
MgO	1.30
SO_3	2.87
K_2O	1.20
Na_2O	0.15
P_2O_5	0.50
Na_2O_{eq}	0.96
S^{2-}	<0.02
Cl^{2-}	0.03

Table 4
Mineralogical composition of cement CEM II/A LL 42.5 R determined by the Bogue calculation.

CEM II/A-LL 42.5 R	Wt.%
C_3S	65.7
C_2S	9.8
C_3A	7.4
C_4AF	11.4

temperature, the maximum temperature rise and the maximum difference between the skin and the core of the structure. They found that, by combining the effects due to the variation of the heat of cement and its dosage, we obtain a variation of 15% on the temperature rise, so 7 °C in our case is possible. Therefore, the increase of the maximum temperature selected for our heat treatment (4 °C) is acceptable. In addition, during the cooling phase, the temperature was gradually reduced from 60 °C to 25 °C over a period of 160 h (the rate is −0.22 °C/h). Then the duration of the heat treatment was 18 days (Fig. 4). Specimens were cured in their molds in a drying oven, and were tightly covered to prevent the evaporation of water during the heat treatment.

In a second time, after observing significant swelling (results will be presented below) in the concrete that has undergone this treatment (with a maximum temperature of 70 °C), it was decided to apply a thermal cycle derived directly from the numerical calculation of the block D, but without changing the maximum temperature reached (Fig. 4). The objective of this is to predict the behavior of the concrete after a heat treatment where the maximum temperature does not exceed 66 °C.

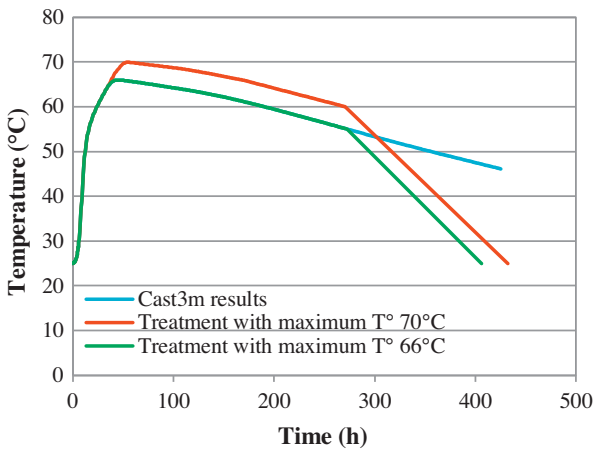

Fig. 4. Experimental applied heat treatments.

After the heat treatments, wetting and drying cycles were applied in accordance with LPC no. 66 pre-test method (LCPC, 2007a). The objective of these cycles is to increase the kinetics of DEF without changing its triggering conditions (Pavoine et al., 2006a, 2006b). Samples are subjected to 2 cycles, each one lasting 14 days. A cycle consists of 7 days of drying at 38 °C and 30% relative humidity, followed by 7 days of immersion in water at 20 °C. Once the cycles are finished, some of concrete specimens were immersed continuously in water, each one in sealed plastic boxes with dimensions slightly larger than specimens to minimize the quantity of water necessary for their immersion, to limit leaching of concrete. On the other hand, three specimens of concrete treated at 70 °C were protected, each one by three coating of aluminum after heat treatment and were kept in air (without being submitted to wetting/drying cycles), in order to stop the water supply. In addition, three specimens were not subjected to the heat treatment to be used as reference. These samples were immersed in water immediately after casting.

The following nomenclature will be used to facilitate discussion of the results:

- *T70-Im* and *T66-Im* for concretes that have been subjected to heat treatments with a maximum temperature of, respectively, 70 °C and 66 °C, and that have been immerged continuously in water;
- *T70-Is* for concrete that have been subjected to a heat treatment with a maximum temperature of 70 °C and that have been isolated from the outside;
- *nt-Im* for concrete that was not heat-treated and that was immersed in water.

3.2. Measurements

A variety of experimental measurements were conducted periodically on concrete specimens. The expansion was measured using an extensometer. For each sample, the length variation was measured on three locations placed at 120° from each other around the diameter. In parallel, the weight was also monitored. In addition, the dynamic elastic modulus was measured by a non-destructive method based on measurement of resonance frequency. This monitoring is carried out using a prototype that measures and records the oscillations of an accelerometer. The procedure consists of exciting the concrete by an impact at the center of one of its bases. The instrument transforms the collected vibrations into electric signals. The resonance frequency is obtained by the measurement of the first longitudinal oscillation frequency, and is linked to the dynamic modulus of the material by the following equation:

$$f_{longi} = \frac{1}{2L}\sqrt{\frac{E_{dyn}}{\rho}} \tag{5}$$

in which f_{longi} is the longitudinal self-oscillation frequency [s^{-1}], L is the height of the specimen [m], E_{dyn} is the dynamic longitudinal elastic modulus [Pa] and ρ is the density of the specimen [kg/m^3].

The frequency of the monitoring of specimens in terms of expansion, weight and dynamic modulus was fixed by a weekly. For each concrete, average of each measurement was computed from three different samples. If later, the behavior shows that the measurement progress slowly, the follow-up is fixed by two weeks or a month.

Additionally, monitoring of mechanical characteristics, porosity and permeability was performed for concretes that were subjected to the heat treatments and that were immersed in water. Five measurements were done on the concrete T70-Im (at the ages of 28, 90, 180, 390 and 640 days), and three measurements on the concrete T66-Im (at the ages of 28, 90 and 180 days). A measurement at the age of 28 days was also performed on the concrete that was not heat-treated to assess the influence of heat treatment on the strength of concrete. Compressive strength and Young's modulus were measured according to NF EN 12390. In parallel, the porosity was obtained by weighing difference between the specimen that have undergone imbibition in water at a pressure of 22 mbar at 20 °C for 48 h and the same specimen dried in an oven at 105 °C (NF P18-459). For the measurement of gas permeability, intrinsic permeability was measured using a Cembureau constant head permeameter with nitrogen as the neutral percolating gas. Each specimen was tested at four differential pressures. For each pressure, the apparent coefficient of permeability k_A (m^2) is calculated from the Hagen–Poiseuille relationship (Kollek, 1989):

$$k_A = \frac{Q}{A}\frac{2\mu L P_{atm}}{(P_i^2 - P_{atm}^2)} \tag{6}$$

in which L is the thickness of the sample (m), A is the cross-sectional area (m^2), Q is the measured gas flow (m^3/s), μ is the coefficient of viscosity (1.76×10^{-5} Pa for nitrogen gas at 20 °C), P_i is the inlet applied pressure (Pa), P_{atm} is the atmospheric pressure (Pa).

Using the Klinkenberg approach, the intrinsic permeability k_V (m^2) relative to viscous flow can be determined by the following relationship:

$$k_A = k_V\left(1 + \frac{b}{P_m}\right) \tag{7}$$

in which $P_m = (P_i + P_{atm})/2$ and b is the Klinkenberg coefficient (Pa).

The determination of k_v and b consists in measuring k_A at different pressures P_i and in plotting it against the inverse of the mean pressure $1/P_m$ (AFPC-AFREM, 1997).

Finally, an analysis of the size distribution of pores by using the technique of mercury intrusion porosimetry was performed in concrete T70-Im. Tests were performed at ages of 90, 390 and 640 days.

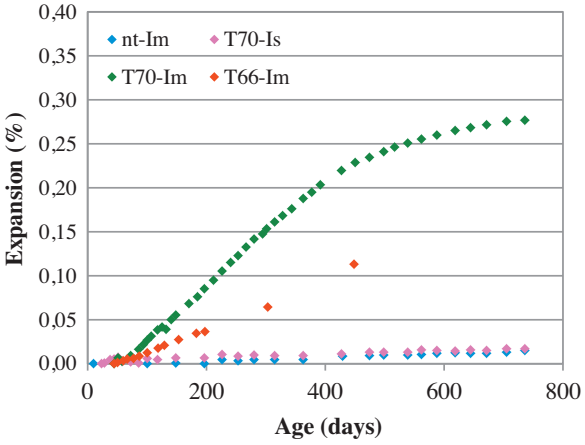

Fig. 5. Swelling of concrete specimens.

4. Results

4.1. Expansion, weight change and mechanical consequences

4.1.1. Expansion and weight change

Fig. 5 shows the expansion versus time data for all the samples of concrete. Only concretes that were subjected to heat treatments and were immersed in water develop swelling, which is due to DEF (using SEM ettringite was observed and there is certainly no development of alkali-aggregate reaction due to the fact that the concrete is made by calcareous aggregates). The speed of swelling in concrete T66-Im is lower than that in concrete T70-Im. This confirms the fact that increasing the value of the maximum temperature reached

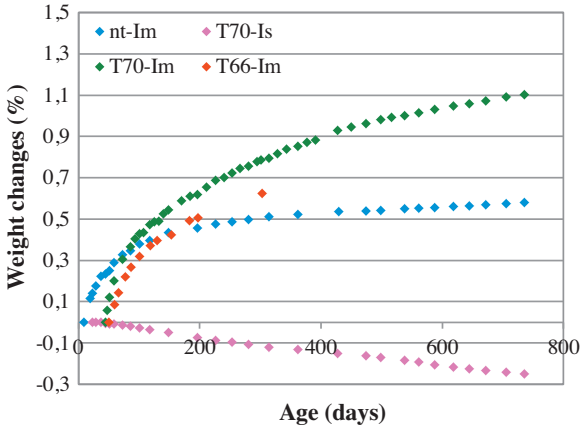

Fig. 6. Weight changes of concrete specimens.

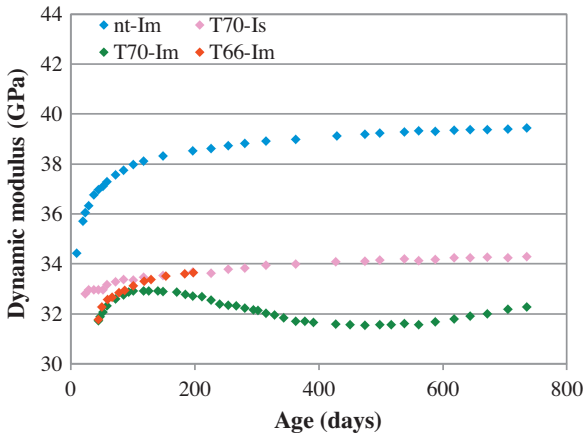

Fig. 7. Evolution of the dynamic modulus of concrete specimens.

during the heat treatment, tends to increase the speed of swelling. It can be seen also that a small difference in the maximum temperature (4 °C) has large effects on the speed of swelling, probably because the temperatures reached are close to the trigger threshold of the DEF. The expansion after 740 days for the concrete T70-Im was about 0.28%. For concrete T66-Im, it was approximately 0.11% at the age of 450 days. The recommendations made by the Technical Guide of LCPC (LCPC, 2007b) propose an expansion threshold of 0.04% at the age of 12 months to highlight significant swelling due to DEF. This threshold was exceeded by the two concretes.

On the other hand, monitoring of the specimens that have not been heat-treated showed that these concretes did not expand during the immersion period. Measured expansion was less than 0.02% at the age of 740 days and is attributed to water absorption during immersion.

Additionally, no significant expansion was recorded for the concrete T70-Is. In parallel, monitoring weight shows a slight loss for this concrete which reaches −0.24% and does not seem to stabilize at the end of our follow-up (Fig. 6). This loss is due to faults in the sealing, especially in areas near the pads of measurement of expansion. This was inevitable despite all precautions taken, but this weight loss is limited, and the core of these samples is probably very little affected by drying. The absence of swelling is due to a lack of water, an essential agent for the reaction of formation of ettringite (one molecule of ettringite contains 32 molecules of water). It is also possible that the absence of swelling can be related to a speed effect. The swelling is not necessarily blocked but can be just retarded because of the absence of alkali leaching due to the absence of external supply of water. Indeed, water also promotes the mobility of agents, and is responsible for leaching of alkali inducing a decrease in pH, which favors the precipitation of ettringite. In case of lack of external water supply, the internal pH of the concrete remains high. Therefore, desorption of sulfate adsorbed on the CSH during the heat treatment is considerably slowed (Divet and Randriambololona, 1998). Under these conditions, the sulfates are less movable and can slow down the kinetics of expansion. Thus, the possibility of a delay and not a blockage of swelling is possible. However, it is currently impossible to know the time needed to reveal the possible first significant accelerations of swelling.

4.1.2. Dynamic modulus of elasticity

Dynamic modulus evolution is presented in Fig. 7. The initial dynamic modulus of concrete non-heat-treated is slightly higher than that of heat-treated concretes. For the non-expanding concretes, the modulus response shows a very slow increase with time. This is due to a slight improvement of the mechanical properties associated with the hydration process of anhydrous cement grains. On the other hand, for the concrete T70-Im, results show a slight increase in dynamic modulus followed by a fall when the expansion reaches around 0.07%. This decrease is observed when the inflection point of the acceleration of the expansion curve is reached, and reflects a slight decrease in mechanical properties of the concrete due to its damage. The end of the decrease in the modulus is observed when the inflection point of the slowdown of the swelling curve is reached. Then, we observe again a new progressive increase of the dynamic modulus. This can be attributed to the closure of cracks by hydration products or by ettringite. The swelling in this phase is probably due to an opening of cracks already existing, and not to the appearance of new cracks. Thus, the evolution of dynamic modulus of concrete affected by DEF is not related to the expansion reached, but to its speed.

Finally, in general, the expansion seems to modify the dynamic modulus very slightly. These results are consistent with those made by Brunetaud (2005) which show that only a sigmoid expansion causes a significant decrease in the modulus.

4.1.3. Effect of swelling on the compressive strength and Young's modulus

Fig. 8 shows a comparison of compressive strength and Young's modulus at the age of 28 days for different concretes. We note, due to heat treatments, a decrease of approximately 20% of the compressive strength. This decrease was observed in both concretes T70-Im and T66-Im. Thus, the application of heat curing induces a lower value of mechanical resistance before the concrete is affected

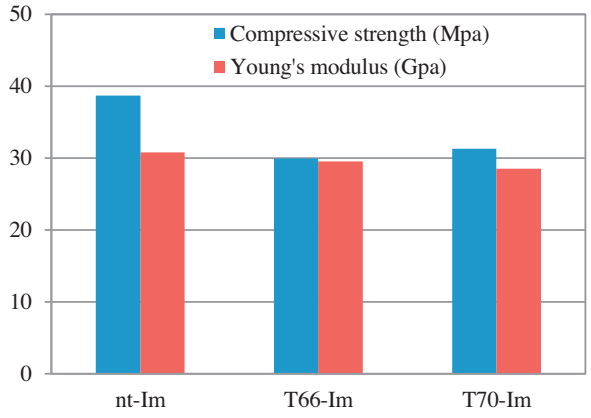

Fig. 8. Effect of heat treatment on the compressive strength and Young's modulus at 28 days.

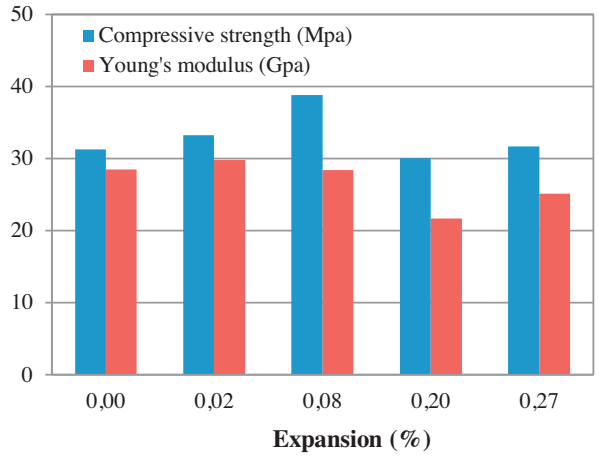

Fig. 9. Relationship between the compressive strength, the Young's modulus and the expansion for concrete T70-Im.

by DEF. However, the Young's modulus does not seem to be affected by the heat treatment. On the other hand, Fig. 9 shows that the concrete T70-Im, which suffers from DEF, presents a degradation of its mechanical properties. We observe a 23% reduction in the compressive strength when the expansion was evolved from 0.08% at the age of 180 days to 0.20% at the age of 390 days. This loss is also observed for the Young's modulus and may be an indicator of the damage of the material. However, the strength loss is not proportional to the expansion reached. In fact, we observe, according to our last measurements (at the age of 640 days when the expansion reaches 0.27%), that the concrete tends to regain a part of its mechanical performance he had lost. This delayed re-increase is observed both on the compressive strength, the dynamic and the Young's modulus. These quantities have a minimum. Minima are observed at around 400 days when the inflection point of the slowdown in the expansion curve is reached (Fig. 10). On the other hand, all measurements on the concrete T66-Im concern only small expansions and the mechanical performances of this concrete was not affected until now (Fig. 11).

4.2. Evolution of permeability with expansion

Fig. 12 shows the evolution of the relative permeability (the ratio between the intrinsic permeability measured at a given time, and that measured at the age of 28 days) with expansion reached for concretes T70-Im and T66-Im. Results show a significant increase in the permeability of the concrete T70-Im. This increase reaches a

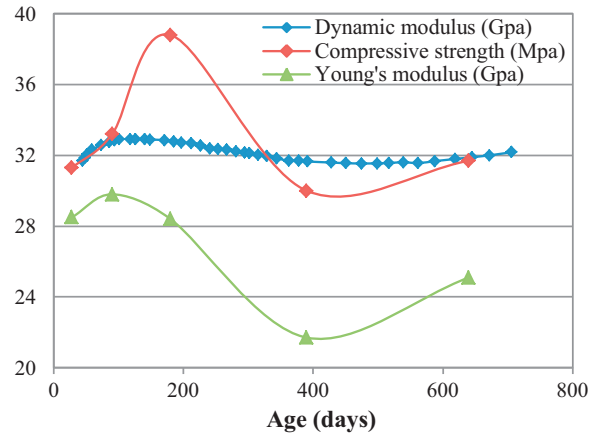

Fig. 10. Mechanical properties versus time for concrete T70-Im.

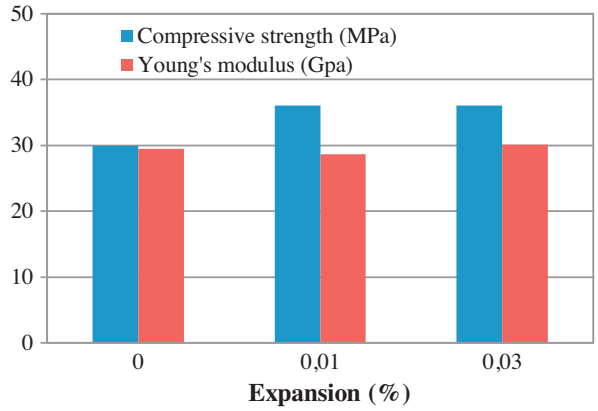

Fig. 11. Relationship between the compressive strength, the Young's modulus and the expansion for concrete T66-Im.

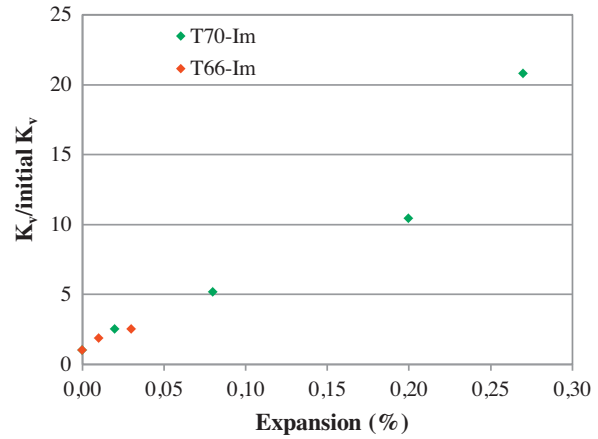

Fig. 12. Relationship between the relative intrinsic permeability and the expansion for concretes T70-Im and T66-Im.

ratio close to 20 when the expansion reaches 0.27%. This is very significant despite the low rate of expansion. This effect is noticeable not only on the intrinsic permeability (calculated from Klinkenberg relationship), but also on the apparent permeability (Fig. 13). Apparent permeabilities measured at any average pressure of gas injection increased after swelling. The increase of permeability reveals a formation of cracks due to swelling, which are able to form a connected network and to create flow paths in the cement

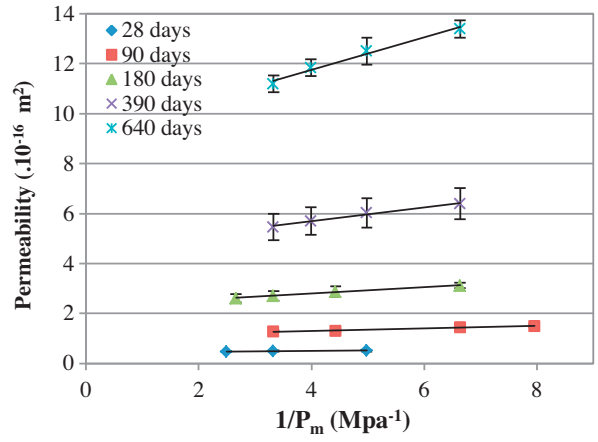

Fig. 13. Effect of the mean gas pressure on the apparent permeability for concrete T70-Im.

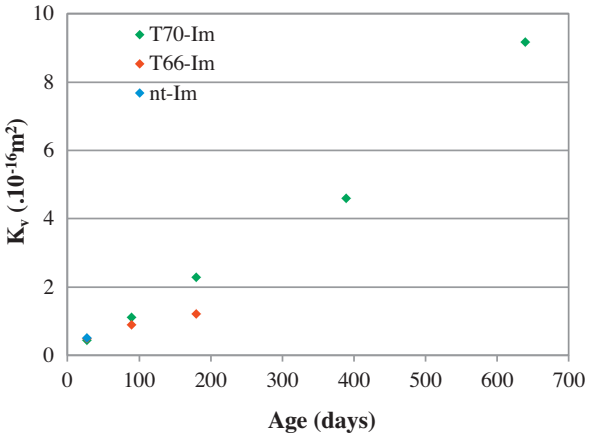

Fig. 14. Intrinsic permeability versus time.

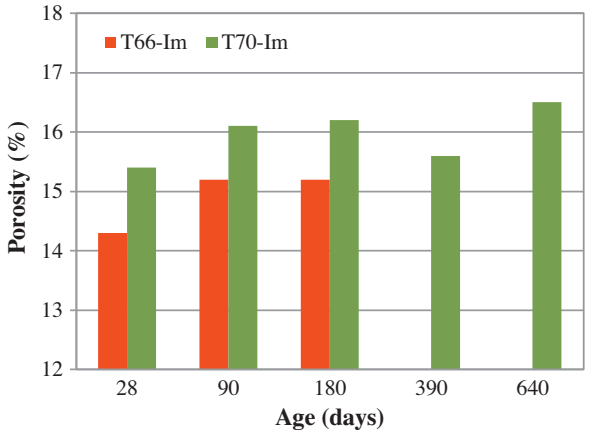

Fig. 15. Porosity of concretes T70-Im and T66-Im versus time.

paste of concrete. In addition, we note that the permeability and the expansion are related by affine relation. Indeed, the evolutions of permeabilities versus expansion for T70-Im and T66-Im are almost identical (Fig. 12). On the other hand, it is possible to note that the initial intrinsic permeability is not sensitive to the applied heat treatments. Indeed, the initial permeabilities, at the age of 28 days, for all samples are equal (Fig. 14). Then, the increase in permeability over time is less important for concrete T66-Im than that of the concrete T70-Im. This is simply due to the fact that the kinetics of the expansion for this one is more important.

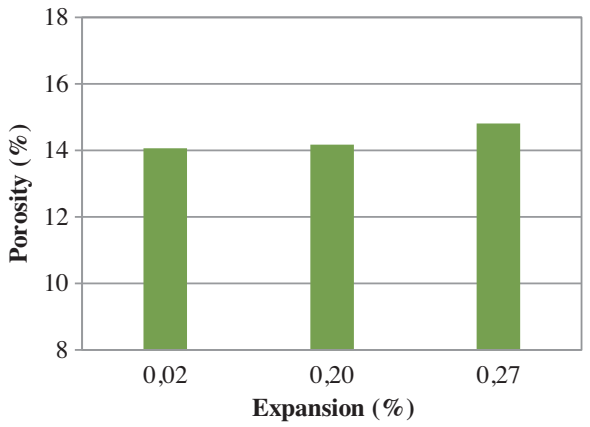

Fig. 16. Relationship between total porosity obtained by mercury porosimetry and expansion for T70-Im.

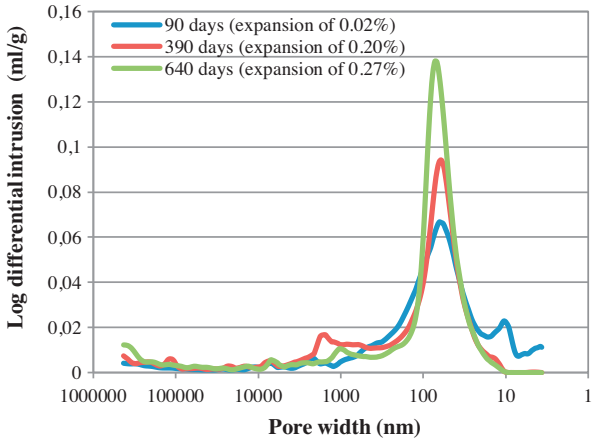

Fig. 17. Differential intruded volume versus pore diameter for T70-Im.

4.3. *Influence of expansion on the porosity and the distribution of the pore size*

The evolution of the total porosity of the concrete T70-Im showed that no significant change was observed after swelling (Fig. 15). These results indicate that, due to the competition between the filling of the existing pores by the ettringite, and the creation of new cracks after swelling, equilibrium was established, and the porosity is thus almost unchanged. The porosity obtained by mercury intrusion porosimetry remains also unchanged (Fig. 16).

Fig. 17 shows the pore size distribution curves. We observe a critical pore width around 65 nm which remains constant after expansion, while its volume increases significantly. This increase can be attributed to microcracking of the cement paste due to constraints imposed by the swelling. We also note a disappearance of pores having a size between 3 and 40 nm, which could correspond to a filling of these pores by ettringite which is formed. A decrease in the volume of pores having a size between 100 and 600 nm was also observed. This reveals a partial filling of these pores and may also be the cause of the increase in the volume of the critical porosity around 65 nm. The increase in the volume of some pores and the filling of others explain the fact that the total porosity was unchanged.

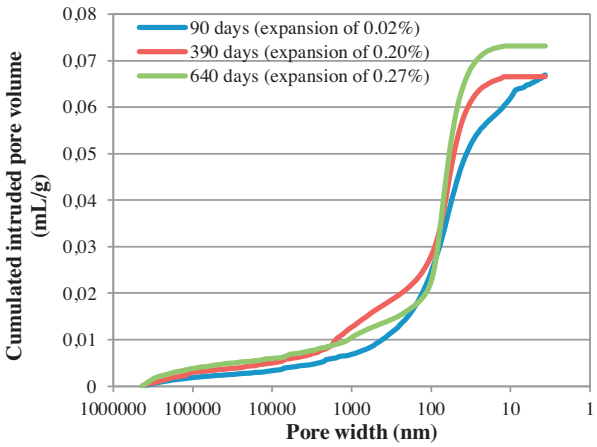

Fig. 18. Relationship between the cumulative intruded pore volume and the pore diameter for T70-Im.

In this case, the swelling does not seem to contribute to a change in the distribution of pore size, but just a volume growth of the main porous mode. Indeed, no significant change in the size of the pores was observed along the swelling. In addition, no shift to larger pores was noted. On the other hand, we observe, after swelling, an increase in the cumulative intruded pore volume for pores size less than 100 nm (Fig. 18). This reveals a porous network more connected than the initial state. These results are in agreement with the evolution of the intrinsic permeability, which show a significant increase of this one.

5. Conclusion

The gas permeability increased significantly after swelling due to delayed ettringite formation in the concrete of the raft foundation of a containment vessel of a nuclear power plant. A linear trend between permeability and swelling was observed. Despite the low rate of expansion (0.28% at 740 days), the permeability was increased with a ratio close to 20 for an expansion that reaches 0.27%. This reveals the development of a connected network of microcracks in the cement paste of concrete. In parallel, the mechanical characterization showed a significant decrease in compressive strength and static modulus, in addition to a decrease due to heat treatment. However, in our case, the porosity was unchanged, and equilibrium has been well established between the pore filling by the ettringite formed and the creation of new cracks.

These results confirm that the risk of DEF development should be considered when the tightness of massive structures could be a factor limiting the service life. Nevertheless, it should be noted that the transposition of the results of this laboratory study to the real evolution of DEF in real structure remains to be studied and will be the theme of a new research project.

References

AFPC-AFREM, 1997. Durabilité des bétons, méthodes recommandés pour la mesure des grandeurs associées à la durabilité, mode opératoire recommandé, essai de perméabilité au gaz du béton durci. Compte-rendu des Journées Techniques de l'AFPC-AFREM, Toulouse.

Baghdadi, N., 2008. Modélisation du couplage chimico-mécanique d'un béton atteint d'une réaction sulfatique interne. PhD thesis. Ecole Nationale des Ponts et Chaussées, Paris, pp. 229.

Barbarulo, R., 2002. Comportement des matériaux cimentaires: action des sulfates et de la température. PhD thesis. Ecole Normale Supérieure de Cachan, Cachan, pp. 272.

Barbarulo, R., Peycelon, H., Prené, S., Marchand, J., 2005. DEF symptoms on mortars induced by high temperature due to cement heat of hydration or late thermal cycle. Cement and Concrete Research 35, 125–131.

Benboudjema, F., Torrenti, J.M., 2008. Early-age behavior of concrete nuclear containments. Nuclear Engineering and Design 238, 2495–2506.

Briffaut, M., Benboudjema, F., Torrenti, J.M., Nahas, G., 2011. Numerical analysis of the thermal active restrained shrinkage ring test to study the early age behavior of massive concrete structures. Engineering Structures 33, 1390–1401.

Brunetaud, X., 2005. Etude de l'influence de différents paramètres et de leurs interactions sur la cinétique et l'amplitude de la réaction sulfatique interne au béton. PhD thesis. Ecole Centrale de Paris, Paris, pp. 265.

Cast3m, 2009. Commissariat à l'Energie Atomique CEA-DEN/DM2S/SEMT. Cast3m finite element code, Available at http://www-cast3m.cea.fr/

Divet, L., 1998. Existe-t-il un risque de développement d'une activité sulfatique endogène dans les pièces de béton de grande masse? Le cas du pont d'Ondes (Haute-Garonne). Bulletin des Laboratoires des Ponts et Chaussées 213, 59–72.

Divet, L., Randriambololona, R., 1998. Delayed ettringite formation: the effect of temperature and basicity on the interaction of sulphate and C-S-H phase. Cement and Concrete Research 28 (3), 357–363.

Divet, L., 2001. Les réactions sulfatiques internes au béton: contribution à l'étude des mécanismes de la formation différée de l'ettringite. Laboratoire Central des Ponts et Chaussées, ERLPC, OA 40., pp. 227.

Hanehara, S., Oyamada, T., Fukuda, S., Fujiwara, T., 2008a. Delayed ettringite formation and alkali aggregate reaction. In: 8th International Conference on Creep, Shrinkage and Durability of Concrete and Concrete Structures, Ise-Shima, Japan, pp. 1051–1056.

Hanehara, S., Oyamada, T., Fujiwara, T., 2008b. Reproduction of delayed ettringite formation in concrete and its mechanism. In: 1st International Conference on Microstructure Related Durability of Cementitious Composites, Nanjing, China, pp. 143–152.

Heinz, D., Ludwig, U., 1987. Mechanism of Secondary Ettringite Formation in Mortars Subjected to Heat Treatment. ACI SP 100, Detroit, USA, pp. 2059–2071.

Kelham, S., 1996. The effect of cement composition and fineness on expansion associated with delayed ettringite formation. Cement and Concrete Composites 18, 171–179.

Kollek, J.J., 1989. The determination of the permeability of concrete to oxygen by the Cembureau method – a recommendation. Materials and Structures 22, 225–230.

Lawrence, C.D., 1995. Mortar expansions due to DEF – effects of curing period and temperature. Cement and Concrete Research 25 (4), 903–914.

Lawrence, C.D., 1999. Long term expansion of mortars and concretes. In: Ettringite – The Sometimes Host of Destruction. ACI SP-177, pp. 105–123.

LCPC, 2007a. Méthode d'essai des lpc n°66: Réactivité d'un béton vis-à-vis d'une réaction sulfatique interne. Techniques et méthodes des laboratoires des ponts et chaussées. Laboratoire Central des Ponts et Chaussées, Paris.

LCPC, 2007b. Recommandations pour la prévention des désordres dus à la réaction sulfatique Interne. Techniques et méthodes des laboratoires des ponts et chaussées. Laboratoire Central des Ponts et Chaussées, Paris.

Odler, I., Chen, Y., 1995. Effect of cement composition on the expansion of heat-cured cement pastes. Cement and Concrete Research 25 (4), 853–862.

Pavoine, A., Divet, L., Fenouillet, S., 2006a. A concrete performance test for delayed ettringite formation: Part I optimization. Cement and Concrete Research 36, 2138–2143.

Pavoine, A., Divet, L., Fenouillet, S., 2006b. A concrete performance test for delayed ettringite formation: Part II validation. Cement and Concrete Research 36, 2144–2151.

Petrov, N., Tagnit-Hamou, A., 2004. Is microcracking really a precursor to DEF and consequent expansion? ACI Materials Journal 101 (6), 442–447.

Scrivener, K.L., Damidot, D., Famy, C., 1999. Possible mechanisms of expansion of concrete exposed to elevated temperatures during curing (also known as DEF) and implications for avoidance of field problems. Cement, Concrete and Aggregates 21 (1), 93–101.

Shayan, A., Ivanusec, I., 1996. An experimental clarification of the association of delayed ettringite formation with alkali-aggregate reaction. Cement and Concrete Composites 18, 161–170.

Torrenti, J.M., Buffo-Lacarrière, L., 2010. On the variability of temperature fields in massive concrete structures at early age. In: 2nd International Symposium on Service Life Design for Infrastructures, Delft.

Tosun, K., 2006. Effect of SO_3 content and fineness on the rate of delayed ettringite formation in heat cured Portland cement mortars. Cement and Concrete Composites 28, 761–772.

Ulm, F.J., Coussy, O., 1998. Couplings in early-age concrete: from material modeling to structural design. International Journal of Solids and Structures 35 (31/32), 4295–4311.

Waller, V., 2000. Relations entre composition des bétons, exothermie en cours de prise et résistance en compression. Collection Etudes et Recherches des Laboratoires des Ponts et Chaussées, série "Ouvrages d'Art". OA35-LCPC, Paris.

Zhang, Z., Olek, J., Diamond, S., 2002. Studies on delayed ettringite formation in early-age, heat-cured mortars. I. Expansion measurements, changes in dynamic modulus of elasticity and weight gains. Cement and Concrete Research 32, 1729–1736.